Article

Highest terrestrial $^3He/^4He$ credibly from the core

https://doi.org/10.1038/s41586-023-06590-8

Received: 30 March 2022

Accepted: 30 August 2023

Published online: 18 October 2023

Check for updates

F. Horton[1]✉, P. D. Asimow[2], K. A. Farley[2], J. Curtice[1], M. D. Kurz[1], J. Blusztajn[1], J. A. Biasi[2,3] & X. M. Boyes[2]

The observation that many lavas associated with mantle plumes have higher $^3He/^4He$ ratios than the upper convecting mantle underpins geophysical, geodynamic and geochemical models of Earth's deep interior. High $^3He/^4He$ ratios are thought to derive from the solar nebula or from solar-wind-irradiated material that became incorporated into Earth during early planetary accretion. Traditionally, this high-$^3He/^4He$ component has been considered intrinsic to the mantle, having avoided outgassing caused by giant impacts and billions of years of mantle convection[1–4]. Here we report the highest magmatic $^3He/^4He$ ratio(67.2 ± 1.8 times the atmospheric ratio) yet measured in terrestrial igneous rocks, in olivines from Baffin Island lavas. We argue that the extremely high-$^3He/^4He$ helium in these lavas might derive from Earth's core[5–9]. The viability of the core hypothesis relaxes the long-standing constraint—based on noble gases in lavas associated with mantle plumes globally—that volatile elements from the solar nebula have survived in the mantle since the early stages of accretion.

High $^3He/^4He$ ratios are closely associated with mantle plumes, but the nature and location of high-$^3He/^4He$ geochemical reservoirs tapped by mantle plumes remains controversial. Possible sources include seismically defined regions in the lowermost mantle[10,11] that may represent some combination of subducted slab graveyards, mantle preserved since planetary accretion and partially degassed mantle[12]. High $^3He/^4He$ ratios in mantle plumes are traditionally attributed to the incomplete outgassing of helium (He) from mantle domains that formed during planetary accretion[13]. Consequently, the upper limit of $^3He/^4He$ observed in mantle-derived rocks has long been considered a constraint for the extent of degassing from ancient mantle domains. The possibility that high-$^3He/^4He$ helium derives from the core[5] potentially relaxes this constraint.

Baffin Island lavas that erupted above the proto-Iceland plume contain olivines with the highest $^3He/^4He$ ratios measured in any terrestrial igneous rocks. There, previously reported ratios extend to 49.8 ± 0.7 times the atmospheric ratio (Ra) of 1.384×10^{-6} (refs. 14,15) in lavas that also contain neon (Ne) more solar-like in isotopic composition than that observed in mid-ocean ridge basalts derived from the convecting upper mantle[16]. However, the $^3He/^4He$ composition of these approximately 62-million-year-old lavas[17] has been strongly modified by post-eruptive radiogenic ^4He ingrowth. For this reason, the magmatic $^3He/^4He$ range in these lavas is difficult to constrain. We expanded on previous studies of Baffin Island lavas by comparing and duplicating $^3He/^4He$ measurements in olivine separates from across individual lava flows and across the accessible lava sequence. Because He stored in olivines dominantly resides in He-rich and uranium–thorium-poor fluid inclusions, it is much less affected by radiogenic ingrowth than He in bulk lavas.

The highest $^3He/^4He$ values we measured, extending to 67.2 ± 1.8 Ra, are significantly higher than previously reported in igneous rocks on Baffin Island or elsewhere[18]. With the aim of linking high $^3He/^4He$ with one or more lithophile element isotopic systems, we assessed magmatic $^3He/^4He$ variability and measured the strontium–neodynium–lead isotopic compositions of the lavas. As we describe below, we found that Baffin Island magmatic $^3He/^4He$ variability may have exceeded 30 Ra and that the highest $^3He/^4He$ ratios are associated with the least radiogenic $^{87}Sr/^{86}Sr$ and most radiogenic $^{143}Nd/^{144}Nd$ geochemical end-member in Baffin Island lavas.

Although we cannot rule out the derivation of high-$^3He/^4He$ helium from mantle sources, below we argue that the core is an equally if not more plausible source. In any case, the He–Ne isotope systematics indicate that high-$^3He/^4He$ helium diffused into the Baffin Island mantle source. Compared with high-$^3He/^4He$ lavas elsewhere, Baffin Island lavas may have uniquely high $^3He/^4He$ because they derive from an especially depleted portion of lowermost mantle; high-$^3He/^4He$ helium that migrated into this reservoir would be better preserved than elsewhere in the mantle.

The highest $^3He/^4He$ lavas are depleted

The measurements reported here (Extended Data Fig. 1) constitute an unusually large He isotopic dataset that (1) rules out in situ cosmogenic ^3He as the source of high $^3He/^4He$ ratios and (2) demonstrates that $^3He/^4He$ ratios exceed 50 Ra in several Baffin Island lavas (Methods and Supplementary Table 1). As conservative estimates of minimum magmatic $^3He/^4He$ ratios, we report averages of the highest reproducible $^3He/^4He$ measurements (defined here as overlapping within 1 s.d. analytical uncertainty) for individual samples. The highest single measured $^3He/^4He$ (90.7 ± 3.9 Ra) was not reproducible, so it is reported for completeness but excluded from the averages (Fig. 1 and Extended Data Table 1). We infer that the highest $^3He/^4He$ component

[1]Geology and Geophysics Department, Woods Hole Oceanographic Institution, Woods Hole, MA, USA. [2]Division of Geological and Planetary Sciences, California Institute of Technology, Pasadena, CA, USA. [3]Present address: Department of Earth Sciences, Dartmouth College, Hanover, NH, USA. ✉e-mail: fhorton@whoi.edu

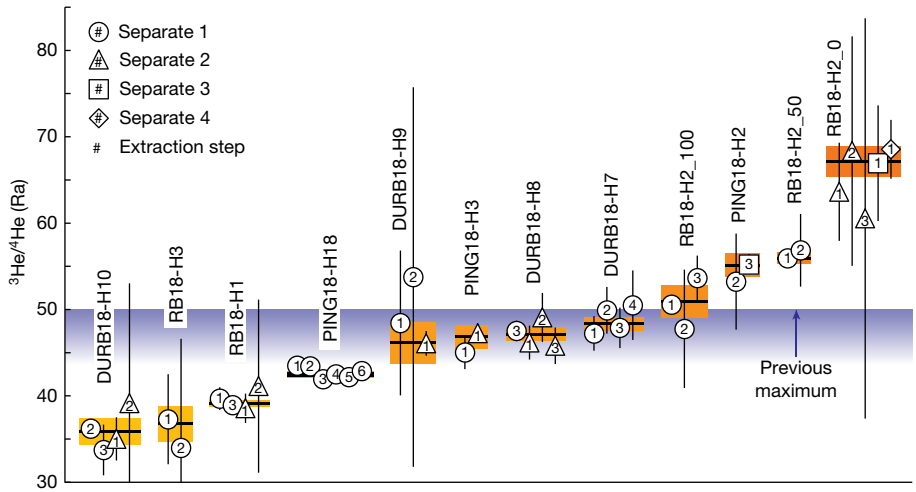

Fig. 1 | Reproducible ^{3}He/^{4}He results. Weighted mean ^{3}He/^{4}He ratios (horizontal black lines) for crushing analyses of Baffin Island olivines that overlap within 1 s.d. analytical uncertainty (vertical black bars) span 30 times the atmospheric ratio (Ra: 1.384×10^{-6}) and in some cases exceed the highest magmatic ^{3}He/^{4}He ratio previously measured in terrestrial igneous rocks (49.8 ± 0.7 Ra)[5,6]. The symbols represent individual crushing extractions from olivine separates. In most cases, the weighted mean ^{3}He/^{4}He represents multiple crush measurements on multiple olivine separates from the same sample. Yellow–orange regions represent weighted 1 s.e. uncertainties for weighted means. See Extended Data Table 1 for weighted means and Supplementary Table 1 for the complete He results.

in the Baffin Island mantle source must exceed the highest of these averages (67.2 ± 1.8 Ra, 1 s.e., $n = 6$).

As previously observed[10,14–16,19–21], Baffin Island olivines show highly variable He abundances and isotopic compositions. The highest reproducible ^{3}He/^{4}He ratios in individual samples range from 35.9 ± 1.5 Ra (1 s.e., $n = 4$) to 67.2 ± 1.8 Ra (1 s.e., $n = 6$). It is unlikely that intrasample reproducibility is due to the coincidental release of similar proportions of radiogenic ^{4}He and mantle He across crushing experiments, so this ^{3}He/^{4}He range probably reflects the minimum magmatic ^{3}He/^{4}He variability across the lava sequence (Methods).

Baffin Island lavas—variably contaminated by continental crust[19]—are mixtures of depleted (low ^{87}Sr/^{86}Sr, low ^{187}Os/^{188}Os and high ^{143}Nd/^{144}Nd) and enriched (high ^{87}Sr/^{86}Sr, high ^{187}Os/^{188}Os and low ^{143}Nd/^{144}Nd) mantle components[22]. The lava flow with the highest reproducible ^{3}He/^{4}He (RB18-H2; 67.2 ± 1.8 Ra) is among the most depleted Baffin Island lavas[15,22] with respect to ^{87}Sr/^{86}Sr (0.70298–0.70306) and ^{143}Nd/^{144}Nd (0.51313–0.51320). These isotopic compositions rule out crustal contamination[19] in this sample and establish that the highest ^{3}He/^{4}He ratios are found in depleted Baffin Island lavas. Besides this observation, however, there are no obvious correlations in the complete dataset between reproducible magmatic ^{3}He/^{4}He and ^{87}Sr/^{86}Sr, ^{143}Nd/^{144}Nd or ^{206,207,208}Pb/^{204}Pb (Supplementary Table 2).

No detectable primordial mantle

Vestiges of gas-rich primordial mantle domains, presumed to be less degassed than other parts of the mantle, are frequently invoked as the source of high ^{3}He/^{4}He ratios in plume-related lavas. Mantle that is less processed and therefore less outgassed than the upper convecting mantle could retain higher ^{3}He/^{4}He (ref. 3). Less processed mantle might exist in seismically defined—and thermochemically distinct—lower mantle regions that supply mantle plumes[23]. When considering helium systematics independently of other isotopic constraints, a small fraction of He-rich (>8×10^{-9} cm^3 ^{3}He g^{-1} at standard temperature and pressure (STP)) primordial mantle in the Baffin Island source could explain the high ^{3}He/^{4}He ratios in the lavas (Fig. 2). However, when the He data are considered in combination with radiogenic isotope systematics, there is no evidence for bulk silicate Earth material with unmodified lithophile element ratios in high-^{3}He/^{4}He mantle[24]. In this study, we highlight two key observations: (1) Baffin Island lavas with the highest ^{3}He/^{4}He ratios have geochemically depleted radiogenic isotope compositions and (2) time-integrated ^{3}He/^{22}Ne ratios of the Baffin Island mantle source are higher than primordial.

Previous He–Sr–Nd isotopic constraints for Baffin Island lavas were already difficult to reconcile with the existence of primordial mantle of bulk silicate Earth composition in the Baffin Island mantle source[14]. Our observation of much higher ^{3}He/^{4}He in lavas with radiogenic isotopic signatures consistent with incompatible element depletion accentuates this problem. Mixtures of depleted mid-ocean ridge mantle (DMM) and

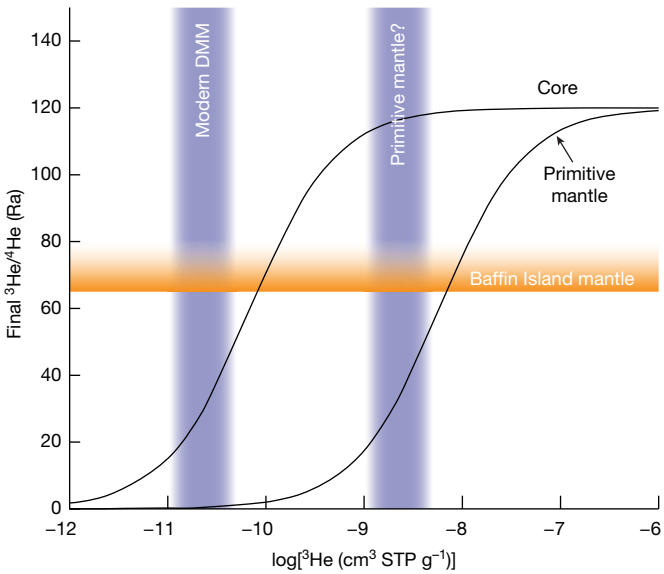

Fig. 2 | Radiogenic ^{4}He ingrowth models. The ^{3}He/^{4}He ratio of theoretical primordial reservoirs today are a function of the ^{3}He concentrations in those reservoirs. Assuming an initial solar-nebula-like ratio (120 Ra) similar to the atmosphere of Jupiter[51] and closed-system behaviour, preservation of >65 Ra requires >8×10^{-9} cm^3 ^{3}He STP g^{-1} in primordial mantle, or only 8×10^{-11} cm^3 ^{3}He STP g^{-1} in the core. Modern depleted mid-ocean ridge basalt mantle (DMM)[52] and theoretical primordial mantle—assumed to be two orders of magnitude greater than DMM—concentrations are shown for reference. The initial thorium and uranium concentrations are assumed to be 100 ng g^{-1} and 52 ng g^{-1}, respectively, in primordial mantle[53] and 2.8 ng g^{-1} and 0.2 ng g^{-1}, respectively, in the core[37].

primordial mantle cannot produce the $^{3}He/^{4}He$, $^{87}Sr/^{86}Sr$, $^{143}Nd/^{144}Nd$ and $^{206}Pb/^{204}Pb$ of the highest $^{3}He/^{4}He$ lava flow (Extended Data Fig. 2), which is more depleted with respect to $^{143}Nd/^{144}Nd$ but more enriched with respect to $^{87}Sr/^{86}Sr$ and $^{206}Pb/^{204}Pb$ than average DMM. Enriched and depleted DMM compositions[25] are also non-viable endmembers. In all cases, $^{87}Sr/^{86}Sr$ and $^{206}Pb/^{204}Pb$ in a Baffin Island depleted endmember would require more primordial mantle or more enriched DMM than permitted by $^{143}Nd/^{144}Nd$. This is true whether primordial mantle was preserved since Earth formation or diluted by mixing into the lower mantle[3]. Any primordial mantle component would need to be small enough to be undetectable in these isotopic systems yet rich enough in ^{3}He to dominate the $^{3}He/^{4}He$ signal.

Furthermore, the time-integrated $^{3}He/^{22}Ne$ composition of the Baffin Island mantle source derived from He–Ne isotope systematics[7] (about 7.5, assuming $^{20}Ne/^{22}Ne = 12.5$) is much higher than the primordial mantle (<2)[23]. High $^{3}He/^{22}Ne$ may be evidence of solubility-controlled magma ocean outgassing events[4]. If so, Baffin Island mantle was intensely degassed like the upper convecting mantle. However, diffusion might also fractionate He and Ne, as discussed below.

Possible ancient mantle origins

Earth formation began with planetesimal growth, continued via planetesimal accretion into planetary embryos and culminated with giant impacts among planetary embryos[26]. During the main phase of accretion, Earth acquired noble gases from the solar nebula, carbonaceous chondrites and solar-wind-irradiated meteoritic material[2]. In high-$^{3}He/^{4}He$ settings, including the Iceland plume, a small number of $^{20}Ne/^{22}Ne$ measurements extend to values higher than in chondrites and solar-wind-irradiated material[13,27]; this is considered evidence of a solar-nebula component. The ^{3}He-rich solar nebula dispersed about 4 Myr after Solar System formation[28] and residual nebular atmospheres around planetary embryos eroded away by 10 Myr (ref. 29), well before the end of the giant-impact stage (the Moon-forming giant impact occurred >30 Myr later[30]). Therefore, the nebular component in Earth was acquired during the earliest stages of accretion. This nebular component survived in Earth, despite giant-impact-induced magma ocean outgassing that could have decreased ^{3}He concentrations in the mantle by four orders of magnitude[31].

A geochemically differentiated basal magma ocean might preserve nebular He and Ne (ref. 1). Like Baffin Island mantle, basal magma ocean cumulates could be geochemically depleted. However, other isotopic constraints preclude ancient geochemical depletion of the Baffin Island source. $^{142}Nd/^{144}Nd$ anomalies (produced by $^{146}Sm \rightarrow ^{142}Nd$, ~100 Myr half-life) in the mantle were mixed away by the end of the Archean[32]. The absence of ^{142}Nd anomalies in mantle-derived lavas since 2 billion years ago[32], including Baffin Island lavas[33], suggests that high-$^{3}He/^{4}He$ lavas are not sourced from depleted mantle reservoirs greater than 4 billion years old.

Alternatively, protoplanetary magma oceans incorporated nebular gases, which were incompletely outgassed and variably overprinted by carbonaceous chondritic gases during later stages of accretion[13,27,34–36]. This might explain why the lower mantle contains a greater nebular component than the upper mantle[13,27]. Importantly, a fraction of nebular gas less than 2% could account for the highest $^{20}Ne/^{22}Ne$ measured in plume-derived lavas, yet would be undetectable with krypton and xenon isotopes, which are mostly of chondritic and recycled origins in the mantle[34]. Thus, nebular gases incorporated into the proto-Earth mantle may have been mostly outgassed and replaced by chondritic gases[2]. If so, the modern mantle preserves nebular and chondritic gas heterogeneities that formed during planetary accretion. The anomalously high $^{3}He/^{4}He$ in Baffin Island lavas might derive from a lower mantle domain with uniquely well preserved nebular He. However, this does not explain the high time-integrated $^{3}He/^{22}Ne$ ratios in Baffin Island lavas relative to the potential sources of gas during accretion (the solar nebula, solar-wind-irradiated material and chondrites), which suggest that solubility-controlled outgassing or diffusion modified the mantle source.

The core as a viable high-$^{3}He/^{4}He$ source

Metal–silicate partitioning experiments suggest that He in the core may be inherited from planetesimals[7] and largely shielded from outgassing during late-stage accretionary processes[31], so the core may be the source of high $^{3}He/^{4}He$ in Baffin Island lavas and elsewhere[5,8,9]. Here we (1) explore whether the core plausibly preserves high $^{3}He/^{4}He$ ratios and solar-like Ne and (2) describe isotopic constraints for other high-$^{3}He/^{4}He$ lavas that support the idea of core material in mantle plumes.

Reasonable ^{3}He concentrations in the core can explain the preservation of high $^{3}He/^{4}He$ ratios for billions of years. If the cores of planetary embryos that formed in the presence of ^{3}He-rich nebular gases avoided complete equilibration with silicate material during late stages of accretion, high concentrations of nebular He could be preserved in Earth's core[7]. Assuming the core initially contained 0.2 ng g^{-1} of uranium and 2.8 ng g^{-1} of thorium[37] and had an initial $^{3}He/^{4}He$ of 120 Ra, preserving $^{3}He/^{4}He > 65$ Ra in the core would require about 8×10^{-11} cm^{3} ^{3}He STP g^{-1} (Fig. 2). If merely 1% of planetesimal core material avoided equilibration during planetary accretion, more than 500 times this required amount of nebular He may exist in the core[7].

The core might also be a source of solar-like Ne. Iron meteorite noble gas abundances indicate that planetesimal cores contained minimally fractionated nebular He and Ne (ref. 6) that could have been incorporated into the terrestrial core. Although He fractionation from Ne can occur in metal–silicate liquid systems analogous to terrestrial magma ocean conditions[38,39], such high-pressure conditions were probably not achieved until after solar-nebula dispersal. In the absence of the nebula, light noble gases would rapidly outgas from a magma ocean and therefore could not sustain fluxes into the core. If we assume that the core incorporated unfractionated nebular He and Ne (ref. 40) from planetesimal cores, $>8 \times 10^{-11}$ cm^{3} ^{3}He STP g^{-1} in the core (enough to satisfy $^{3}He/^{4}He$ constraints) corresponds to $>3 \times 10^{-10}$ cm^{3} STP g^{-1} of Ne. Neon production in the core is probably dominated by α-particle collisions with oxygen, even though the core contains only 2–4 wt% oxygen[41]. Assuming closed-system behaviour, the nucleogenic component would not detectably influence Ne isotopic ratios in the core over 4.5 Gyr, even assuming upper limit oxygen[41], uranium and thorium concentration estimates[37] (Methods).

Other isotopic systems lend credence to the idea that the core is the source of He in plume-related lavas. Some high-$^{3}He/^{4}He$ lavas have $^{182}W/^{184}W$ anomalies generated by $^{182}Hf \rightarrow ^{182}W$ decay (~9 Myr half-life) during the first 60 Myr of Solar System history, implying that high-$^{3}He/^{4}He$ helium derives from one or more domains (perhaps the core) preserved since the early Hadean[42,43]. Iceland lavas with anomalously light tungsten and high $^{3}He/^{4}He$ ratios (up to 25 Ra) have sulfur isotopic compositions that converge towards chondritic ratios[44]. This may be consistent with primordial tungsten, sulfur, Ne and He transfer from the core into the Iceland mantle plume.

Since the discovery of high $^{3}He/^{4}He$ ratios in lavas associated with mantle plumes[45], most mantle mixing models have assumed the survival of ancient high-$^{3}He/^{4}He$ material in the mantle[4], despite calculations that modern convection rates would destroy large-scale heterogeneities in less than the age of Earth[46]. By relaxing this constraint, the core hypothesis permits geodynamic models in which mantle heterogeneities that formed during the main stages of planetary accretion need not have survived.

Core–mantle exchange mechanisms

Helium–neon systematics in Baffin Island lavas have two key implications for the origins of the high $^{3}He/^{4}He$ ratios in Baffin Island lavas and

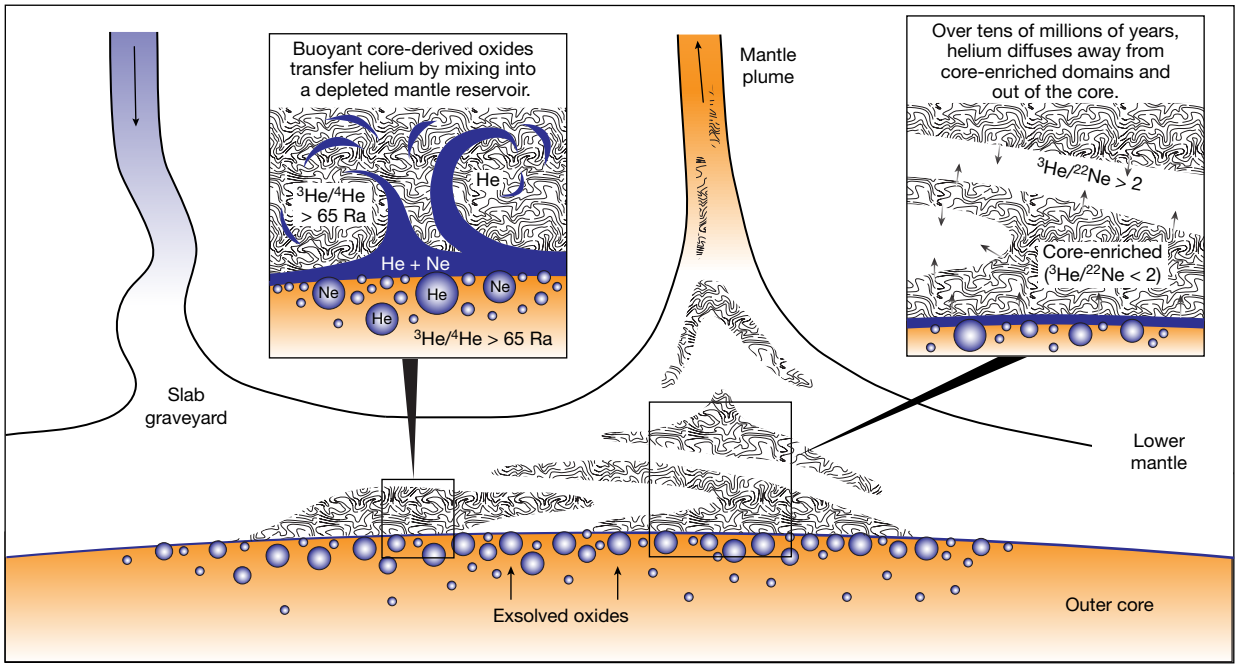

Fig. 3 | Schematic illustration of core-to-plume transfer. Buoyant exsolved oxides from the outer core may mix into a lowermost mantle reservoir composed of subducted depleted mantle (that is, a slab graveyard). Mantle enriched by core-derived material might inherit high ^{3}He/^{4}He from the core. Over tens of millions of years, core-derived He may then diffuse into the surrounding depleted mantle. Both domains—one enriched by core-derived oxides, the other by He diffusion—may become incorporated into mantle plumes, like the Iceland plume that produced the Baffin Island lavas.

elsewhere. First, the presence of solar-nebula-like Ne in high-^{3}He/^{4}He lavas globally suggests that nebula-like Ne and high-^{3}He/^{4}He helium in mantle plumes have a common origin. Neon in Baffin Island olivines[16] is a mixture of modern atmospheric contamination and mantle gas with a ^{21}Ne/^{22}Ne ratio of 0.0368 ± 0.001 when extrapolated to a solar ^{20}Ne/^{22}Ne ratio of 13.36 ± 0.09 (ref. 25). This component in Baffin Island lavas—like mantle components in Galapagos, Iceland and Hawai'i lavas—is intermediate between solar (<0.03282) and mid-ocean ridge basalt (>0.055) ^{21}Ne/^{22}Ne ratios[4,40], implying that Baffin Island mantle contains more nebular Ne than the convecting upper mantle but is more nucleogenic than expected for the core. Thus, the Ne in Baffin Island lavas was not derived exclusively from the core. Rather, it may be a mixture of nebular Ne from the core, chondritic Ne accreted into the mantle and recycled Ne derived from seawater[27,36].

Baffin Island time-integrated ^{3}He/^{22}Ne ratios provide a second key constraint. Neither ^{3}He nor ^{22}Ne are produced in significant quantities in Earth, so deviations from primordial ^{3}He/^{22}Ne ratios imply fractionation of He from Ne. The higher time-integrated ^{3}He/^{22}Ne in Baffin Island mantle (approximately 7.5 or 10 assuming ^{20}Ne/^{22}Ne of 12.5 or 13.8, respectively[4,16]) than in Iceland mantle, primordial mantle, the solar nebula and solar wind[4] implies that that nebular Ne and He are decoupled in the Baffin Island source.

Faster diffusion of He compared with Ne in the mantle might explain the higher Baffin Island ^{3}He/^{22}Ne. Helium diffusion across kilometres of the lowermost mantle is plausible over tens of millions of years. Although there is a dearth of information about He diffusion in lower mantle phases such as bridgmanite, extrapolation of experimental[47] and theoretical[48] olivine diffusivities to 4,000 K suggests that the He diffusion length scales ($\sqrt{Dt}$, where D is diffusivity and t is time) are on the order of kilometres over tens of millions of years. By contrast, Ne diffusion through silicate minerals is five orders of magnitude slower than He in the upper mantle[49]. Neon and He have similar activation energies in olivine[48,49] and therefore might have similar relative diffusivities throughout the silicate mantle. If rapid He diffusion relative to Ne applies to lower mantle phases, He–Ne separation may occur over the greatest distances in the deepest portion of the mantle (that is, nearest the core) because, to first order, diffusion rates scale with temperature. Likewise, He and tungsten from the core may be fractionated by diffusion at the base of the mantle[8].

Helium diffusion from the core (or ancient high-^{3}He/^{4}He mantle) might imprint a high-^{3}He/^{4}He signature on geochemically depleted mantle domains. This might explain the elevated ^{3}He/^{22}Ne and ^{3}He/^{4}He ratios in the Baffin Island mantle source, as well as the lack of ^{3}He/^{4}He correlation with strontium, neodymium and lead isotopic ratios. However, if Ne diffusion is limited to scales of perhaps metres or less throughout the mantle, then diffusion is an unlikely mechanism for solar-like Ne transfer into the Baffin Island mantle source.

Thus, the high ^{3}He/^{4}He, high ^{3}He/^{22}Ne and nebula-like Ne in Baffin Island mantle cannot simultaneously be explained by (1) direct assimilation of core into depleted mantle, or (2) diffusion of gases from the core into depleted mantle. The same holds true for the assimilation of, or the diffusion of gases out of, ancient high-^{3}He/^{4}He mantle. We propose a hybrid scenario in which Baffin Island mantle contains both core-derived material and He-infused mantle (Fig. 3). The lack of siderophile element enrichments in plume lavas[43] implies that bulk core does not mix into mantle plumes, but buoyant oxides exsolved from the outer core could be conveyors of He[9] and perhaps other noble gases.

Fluxes of heavy noble gases from the core into plume source mantle may be undetectable. The majority of xenon and krypton in plumes derives from recycled seawater and atmosphere[34,35]. The remainder is nearly all chondritic and lacks the detectable solar-nebula component apparent in plume Ne[13,27]. Percentage levels of nebular gases would be detectable with Ne but not krypton and xenon isotopes[34]. Thus, the nebular gas component in the mantle may derive from the core and locally overprint an intrinsic chondritic component. If so, He and Ne—rich in the solar nebula and highly susceptible to mantle outgassing—could be the most sensitive tracers of nebular gases from the core.

Core-derived He and Ne isotopic anomalies may be uniquely well preserved in plume mantle because large chemical and isotopic gradients exist across the core–mantle boundary for these elements.

Compared with high-^{3}He/^{4}He lavas elsewhere, Baffin Island lavas may have anomalously high ^{3}He/^{4}He ratios because they derive from an especially depleted (that is, initially poor in ^{4}He and ^{21}Ne, as well as uranium and thorium) portion of lowermost mantle. High-^{3}He/^{4}He helium that migrated into this reservoir would be better preserved than elsewhere in the mantle. For example, oceanic mantle lithosphere subducted into a slab graveyard at the core–mantle boundary[12,50] and then entrained in a mantle plume could have conveyed core-derived He to Earth's surface.

Online content

Any methods, additional references, Nature Portfolio reporting summaries, source data, extended data, supplementary information, acknowledgements, peer review information; details of author contributions and competing interests; and statements of data and code availability are available at https://doi.org/10.1038/s41586-023-06590-8.

1. Coltice, N., Moreira, M., Hernlund, J. & Labrosse, S. Crystallization of a basal magma ocean recorded by helium and neon. *Earth Planet. Sci. Lett.* **308**, 193–199 (2011).
2. Mukhopadhyay, S. & Parai, R. Noble gases: a record of Earth's evolution and mantle dynamics. *Annu. Rev. Earth Planet. Sci.* **47**, 389–419 (2019).
3. Gonnermann, H. M. & Mukhopadhyay, S. Preserving noble gases in a convecting mantle. *Nature* **459**, 560–563 (2009).
4. Tucker, J. M. & Mukhopadhyay, S. Evidence for multiple magma ocean outgassing and atmospheric loss episodes from mantle noble gases. *Earth Planet. Sci. Lett.* **393**, 254–265 (2014).
5. Porcelli, D. & Halliday, A. N. The core as a possible source of mantle helium. *Earth Planet. Sci. Lett.* **192**, 45–56 (2001).
6. Vogt, M., Trieloff, M., Ott, U., Hopp, J. & Schwarz, W. H. Solar noble gases in an iron meteorite indicate terrestrial mantle signatures derive from Earth's core. *Commun. Earth Environ.* **2**, 92 (2021).
7. Roth, A. S. et al. The primordial He budget of the Earth set by percolative core formation in planetesimals. *Geochem. Perspect. Lett.* **9**, 26–31 (2019).
8. Ferrick, A. L. & Korenaga, J. Long-term core–mantle interaction explains W–He isotope heterogeneities. *Proc. Natl Acad. Sci. USA* **120**, e2215903120 (2023).
9. Deng, J. & Du, Z. Primordial helium extracted from the Earth's core through magnesium oxide exsolution. *Nat. Geosci.* **16**, 541–545 (2023).
10. Rizo, H. et al. Preservation of Earth-forming events in the tungsten isotopic composition of modern flood basalts. *Science* **352**, 809–812 (2016).
11. White, W. M. Isotopes, DUPAL, LLSVPs, and anekantavada. *Chem. Geol.* **419**, 10–28 (2015).
12. Jones, T. D., Sime, N. & van Keken, P. E. Burying Earth's primitive mantle in the slab graveyard. *Geochem. Geophys. Geosyst.* **22**, e2020GC009396 (2021).
13. Mukhopadhyay, S. Early differentiation and volatile accretion recorded in deep-mantle neon and xenon. *Nature* **486**, 101–104 (2012).
14. Stuart, F. M., Lass-Evans, S., Fitton, J. G. & Ellam, R. M. High ^{3}He/^{4}He ratios in picritic basalts from Baffin Island and the role of a mixed reservoir in mantle plumes. *Nature* **424**, 57–59 (2003).
15. Starkey, N. A. et al. Helium isotopes in early Iceland plume picrites: constraints on the composition of high ^{3}He/^{4}He mantle. *Earth Planet. Sci. Lett.* **277**, 91–100 (2009).
16. Horton, F. et al. Primordial neon in high-^{3}He/^{4}He Baffin Island olivines. *Earth Planet. Sci. Lett.* **558**, 116762 (2021).
17. Biasi, J., Asimow, P. D., Horton, F. & Boyes, X. M. Eruption rates, tempo, and stratigraphy of Paleocene flood basalts on Baffin Island, Canada. *Geochem. Geophys. Geosyst.* **23**, e221GC010172 (2022).
18. Jackson, M. G., Konter, J. G. & Becker, T. W. Primordial helium entrained by the hottest mantle plumes. *Nature* **542**, 340–343 (2017).
19. Willhite, L. N. et al. Hot and heterogenous high-^{3}He/^{4}He components: new constraints from proto-iceland plume lavas from Baffin Island. *Geochem. Geophys. Geosyst.* **20**, 5939–5967 (2019).
20. Graham, D. W. et al. Helium isotope composition of the early Iceland mantle plume inferred from the Tertiary picrites of West Greenland. *Earth Planet. Sci. Lett.* **160**, 241–255 (1998).
21. Jackson, M. G. et al. Evidence for the survival of the oldest terrestrial mantle reservoir. *Nature* **466**, 853–856 (2010).
22. Kent, A. J. R. et al. Mantle heterogeneity during the formation of the North Atlantic igneous province: constraints from trace element and Sr–Nd–Os–O isotope systematics of Baffin Island picrites. *Geochem. Geophys. Geosyst.* **5**, Q11004 (2004).
23. Jones, T. D., Davies, D. R. & Sossi, P. A. Tungsten isotopes in mantle plumes: heads it's positive, tails it's negative. *Earth Planet. Sci. Lett.* **506**, 255–267 (2019).
24. Porcelli, D. & Ballentine, C. J. Models for distribution of terrestrial noble gases and evolution of the atmosphere. *Rev. Mineral. Geochem.* **47**, 411–480 (2002).
25. Workman, R. K. & Hart, S. R. Major and trace element composition of the depleted MORB mantle (DMM). *Earth Planet. Sci. Lett.* **231**, 53–72 (2005).
26. Halliday, A. N. & Canup, R. M. The accretion of planet Earth. *Nat. Rev. Earth Environ.* **4**, 19–35 (2022).
27. Williams, C. D. & Mukhopadhyay, S. Capture of nebular gases during Earth's accretion is preserved in deep-mantle neon. *Nature* **565**, 78–81 (2019).
28. Weiss, B. P., Bai, X.-N. & Fu, R. R. History of the solar nebula from meteorite paleomagnetism. *Sci. Adv.* https://doi.org/10.1126/sciadv.aba5967 (2021).
29. Olson, P. L. & Sharp, Z. D. Nebular atmosphere to magma ocean: a model for volatile capture during Earth accretion. *Phys. Earth Planet. Inter.* **294**, 106294 (2019).
30. Thiemens, M. M., Sprung, P., Fonseca, R. O. C., Leitzke, F. P. & Münker, C. Early Moon formation inferred from hafnium–tungsten systematics. *Nat. Geosci.* **12**, 696–700 (2019).
31. Wang, K., Lu, X., Liu, X., Zhou, M. & Yin, K. Partitioning of noble gases (He, Ne, Ar, Kr, Xe) during Earth's core segregation: a possible core reservoir for primordial noble gases. *Geochim. Cosmochim. Acta* https://doi.org/10.1016/j.gca.2022.01.009 (2022).
32. Hyung, E. & Jacobsen, S. B. The ^{142}Nd/^{144}Nd variations in mantle-derived rocks provide constraints on the stirring rate of the mantle from the Hadean to the present. *Proc. Natl Acad. Sci. USA* **117**, 14738–14744 (2020).
33. de Leeuw, G. A. M., Ellam, R. M., Stuart, F. M. & Carlson, R. W. ^{142}Nd/^{144}Nd inferences on the nature and origin of the source of high ^{3}He/^{4}He magmas. *Earth Planet. Sci. Lett.* **472**, 62–68 (2017).
34. Broadley, M. W. et al. Identification of chondritic krypton and xenon in Yellowstone gases and the timing of terrestrial volatile accretion. *Proc. Natl Acad. Sci. USA* **117**, 13997–14004 (2020).
35. Péron, S., Mukhopadhyay, S., Kurz, M. D. & Graham, D. W. Deep-mantle krypton reveals Earth's early accretion of carbonaceous matter. *Nature* **600**, 462–467 (2021).
36. Parai, R. A dry ancient plume mantle from noble gas isotopes. *Proc. Natl Acad. Sci. USA* **119**, e2201815119 (2022).
37. Yuan, L. & Steinle-Neumann, G. The helium elemental and isotopic compositions of the Earth's core based on ab initio simulations. *J. Geophys. Res. Solid Earth* **126**, e2021JB023106 (2021).
38. Li, Y., Vočadlo, L., Ballentine, C. & Brodholt, J. P. Primitive noble gases sampled from ocean island basalts cannot be from the Earth's core. *Nat. Commun.* **13**, 3770 (2022).
39. Bouhifd, M. A., Jephcoat, A. P., Porcelli, D., Kelley, S. P. & Marty, B. Potential of Earth's core as a reservoir for noble gases: case for helium and neon. *Geochem. Perspect. Lett.* **15**, 15–18 (2020).
40. Heber, V. S. et al. Isotopic mass fractionation of solar wind: evidence from fast and slow solar wind collected by the Genesis mission. *Astrophys. J.* **759**, 121 (2012).
41. Faure, P. et al. Uranium and thorium partitioning in the bulk silicate Earth and the oxygen content of Earth's core. *Geochim. Cosmochim. Acta* **275**, 83–98 (2020).
42. Mundl-Petermeier, A. et al. Temporal evolution of primordial tungsten-182 and ^{3}He/^{4}He signatures in the Iceland mantle plume. *Chem. Geol.* **525**, 245–259 (2019).
43. Mundl-Petermeier, A. et al. Anomalous ^{182}W in high ^{3}He/^{4}He ocean island basalts: fingerprints of Earth's core? *Geochim. Cosmochim. Acta* **271**, 194–211 (2020).
44. Ranta, E. et al. Ancient and recycled sulfur sampled by the Iceland mantle plume. *Earth Planet. Sci. Lett.* **584**, 117452 (2022).
45. Kurz, M. D., Jenkins, W. J. & Hart, S. R. Helium isotopic systematics of oceanic islands and mantle heterogeneity. *Nature* **297**, 43–47 (1982).
46. Hoffman, N. R. A. & McKenzie, D. P. The destruction of geochemical heterogeneities by differential fluid motions during mantle convection. *Geophys. J. Int.* **82**, 163–206 (1985).
47. Hart, S. R., Kurz, M. D. & Wang, Z. Scale length of mantle heterogeneities: constraints from helium diffusion. *Earth Planet. Sci. Lett.* **269**, 508–517 (2008).
48. Wang, K., Brodholt, J. & Lu, X. Helium diffusion in olivine based on first principles calculations. *Geochim. Cosmochim. Acta* **156**, 145–153 (2015).
49. Cherniak, D. J., Thomas, J. B. & Watson, E. B. Neon diffusion in olivine and quartz. *Chem. Geol.* **371**, 68–82 (2014).
50. Schaefer, B. F., Turner, S., Parkinson, I., Rogers, N. & Hawkesworth, C. Evidence for recycled Archaean oceanic mantle lithosphere in the Azores plume. *Nature* **420**, 304–307 (2002).
51. Atreya, S. K., Mahaffy, P. R., Niemann, H. B., Wong, M. H. & Owen, T. C. Composition and origin of the atmosphere of Jupiter—an update, and implications for the extrasolar giant planets. *Planet. Space Sci.* **51**, 105–112 (2003).
52. Moreira, M. A. & Kurz, M. D. In *The Noble Gases as Geochemical Tracers. Advances in Isotope Geochemistry* (ed. Burnard, P.) 371–391 (Springer, 2013).
53. McDonough, W. F. & Sun, S. S. The composition of the Earth. *Chem. Geol.* **120**, 223–253 (1995).

Methods

Noble gas analysis

Twenty-five picrite samples were selected for He isotopic analysis from across Durban Island, Padloping Island and Cumberland Peninsula on the mainland of Baffin Island (Supplementary Table 1). These include five samples previously reported in ref. 16. The samples were collected from cliff faces where they were well shielded from cosmic rays. Three of the samples (RB18-H2_0, RB18-H2_50 and RB18-H2_100) are from 0 cm, 50 cm and 100 cm above the base of a single lava flow (Extended Data Fig. 3), where they were shielded beneath overhanging rock. The largest matrix-free olivines were handpicked from the >0.5 mm sieved fractions of crushed samples and ultrasonically cleaned in ethanol baths at 25 °C. To assess the reproducibility of the results, multiple olivine separates were analysed for 16 of the samples. Some olivines in sample PING18-H18 have distinct inclusion populations (either fluid-inclusion rich or spinel-inclusion rich), so we analysed randomly selected olivines (separate 1), spinel-rich olivines (separate 2) and fluid-inclusion-rich olivines (separate 3) independently.

Gases from multiple extraction steps (vacuum crushing and fusion) were measured for nearly all the separates. Helium was extracted from up to four olivine separates per sample. Crushing consisted of one to seven sequential extraction steps per olivine separate. Selected crush residues were then fused to extract all residual He. Combined, these totalled 135 analyses excluding blanks and standards. To cross-check the results, analyses were carried out at California Institute of Technology (Caltech) and Woods Hole Oceanographic Institution (WHOI).

At WHOI, olivine separates were ultrasonically rinsed in acetone and loaded into cylindrical ultrahigh vacuum crushing chambers. Before rinsing, one separate (PING18-H2 separate 3) was chemically etched in fluoroboric acid for 60 min. A magnetic sphere was manually actuated to crush the olivines using between 1 and 40 strokes per analysis. Multiple crushing analyses were performed on each olivine separate, but only those that yielded He in excess of blank measurements are reported. Extracted gases were purified on bulk titanium sponge and zirconium–iron–aluminium pellet getters. Helium was sorbed and desorbed on a charcoal cryotrap and analysed on a MAP 215-50 magnetic sector mass spectrometer. Line blanks had ^{4}He less than 2×10^{-11} cm^3 STP. Procedural blanks had ^{3}He/^{4}He < 5 Ra and ^{4}He less than 2×10^{-11} cm^3 STP, except for 2 crushers that yielded 2×10^{-10}–6×10^{-10} cm^3 STP (these high-blank crushers were used for analyses of samples DURB18-H1, PING18-H14 and PING18-H26, and are indicated in Supplementary Table 1). Fractions of the crush residue were fused in a double vacuum furnace at 1,550 °C to extract any remaining He, which was analysed by the same methods. After making blank and interference corrections, we normalized to in-house mid-ocean ridge basalt gas standards (8.36 ± 0.07 Ra), as described in refs. 54,55. When samples yielded high quantities of He, samples were split to fractions similar in size to the in-house standard (about 5×10^{-9} cm^3 STP). We minimized the effect of signal-dependent sensitivity by maintaining ^{4}He signals within a factor of four of the standards. On the basis of the long-term reproducibility of standards of variable sizes, signal-dependent sensitivity influenced the highest ^{3}He/^{4}He ratios by <0.1 Ra.

Samples were analysed at Caltech using the crusher apparatus and procedures described previously[56] except that measurements were performed on a Helix SFT mass spectrometer. Automated crushing for the time periods utilized at Caltech is more complete than the more gradual manual crushing at WHOI, apparently contributing to greater extraction of matrix-hosted radiogenic He.

Crushing and fusion of Baffin Island olivines yielded 0.012×10^{-9}–65×10^{-9} cm^3 ^{4}He STP g^{-1} and 2×10^{-9}–41×10^{-9} cm^3 ^{4}He STP g^{-1} per analysis, respectively, and ^{3}He/^{4}He of 2.3–91 Ra and 0.36–44 Ra, respectively (Supplementary Table 1). The highest measured ^{3}He/^{4}He (90.7 ± 3.9 Ra for sample PING18-H2) far exceeds any others (Extended Data Fig. 1) but was unreproducible. Nothing about the standards, blanks or signal size causes us to question the validity of this measurement. Crushing experiments performed on two additional mineral separates from this sample yielded average ^{3}He/^{4}He of 51 Ra and 41 Ra (n = 3 for each). For these and nearly all mineral separates, repeated crushing steps of the same aliquot yielded successively lower ^{3}He/^{4}He ratios (Extended Data Fig. 4), implying that post-eruptive radiogenic He constituted a greater fraction of the released gas as crushing progressed and grain size decreased. This is a well known behaviour[57]. There was either extreme isotopic variability within this sample or unidentified analytical problems.

We report inverse-variance weighted means and weighted standard errors for the maximum reproducible ^{3}He/^{4}He ratios within and among separates of 12 samples (Extended Data Table 1). We consider ^{3}He/^{4}He results reproducible when uncertainties overlap within 1 s.d. Sample RB18-H2_0 yielded the highest reproducible ^{3}He/^{4}He of 67.2 ± 1.8 Ra (1 s.e.); this is the average of the 6 highest ^{3}He/^{4}He results—which are presumed to have the smallest radiogenic ^{4}He contributions—of 12 total crushing measurements made on 4 different olivine separates in 2 different laboratories.

The fusion measurements yielded similar or lower ^{3}He/^{4}He ratios compared with crushing measurements (Extended Data Fig. 2), which is inconsistent with the presence of significant cosmogenic He in this sample suite. Rather, the fusion results imply that some samples have >2.5×10^{-8} cm^3 STP g^{-1} of radiogenic ^{4}He, constituting greater than 95% of the total ^{4}He per sample in the most extreme cases. Thus, radiogenic ^{4}He—rather than cosmogenic ^{3}He—that accumulated since eruption in melt inclusions and the olivine lattice can explain much of the isotopic variability we observe across multiple crush steps and fusion results of individual samples.

Electron microprobe

To assess links between olivine crystal chemistry and inclusion population, we performed electron microprobe transects across nine olivine crystals (four with abundant fluid inclusions and five with spinel inclusions) from sample PING18-H2. The olivines were mounted in epoxy and polished to approximately halfway through each grain. On a JEOL JXA-8200 Superprobe, 2 perpendicular 10-point transects were conducted on each grain, using an accelerating voltage of 15 kV that corresponds to an approximately 1-μm interaction volume. Counting errors of X-ray intensities were less than 1% for silicon, calcium, iron, magnesium and nickel and less than 5% for chromium, manganese and aluminium. The results are reported in Supplementary Table 3.

^{3}He/^{4}He variability

Olivine chemistry, inclusion populations and He measurements constrain Baffin Island intrasample, intraflow and interflow ^{3}He/^{4}He variability. Differences in olivine chemistry and inclusion populations provide useful petrologic context for interpreting our He isotopic results. Some Baffin Island lavas (most notably PING18-H18 and DURB18-H7) contain olivines with abundant fluid inclusions. We closely examined PING18-H18, which contains normally zoned olivines with spinel-rich cores and fluid-inclusion-rich rims (Extended Data Figs. 5 and 6). This zoning indicates that fluid-inclusion-rich olivine domains grew in more evolved magmas than the spinel-rich cores.

^{3}He/^{4}He measurements obtained by crushing of a fluid-inclusion-rich olivine separate (PING18-H18, separate 3) provide insight about magmatic isotopic variability (Supplementary Table 1). This separate yielded about 30 times higher ^{4}He per gram than spinel-rich olivines (separate 2) from the same sample. ^{3}He/^{4}He measured during crushing of separate 3 vary by >8 Ra (about 42–50 Ra). Yet, unlike all other mineral separates in this study, the fusion ^{3}He/^{4}He ratio of this separate (43.7 ± 0.7 Ra) was indistinguishable from the total He released

by crushing (41.6 ± 4.7). Thus, radiogenic ^{4}He comprised a negligible fraction of the total He and cannot explain the observed ^{3}He/^{4}He variability. We infer that intrasample magmatic ^{3}He/^{4}He variability (in this sample and others) may exceed 8 Ra but is averaged out during some bulk crushing experiments (for example, PING18-H18 separate 1 and PING18-H2 separate 1).

Even more isotopic variability is observed across a single lava flow. Compared with RB18-H2_0 (67.2 ± 1.8 Ra), two samples collected immediately above (Extended Data Fig. 4) yielded lower ^{3}He/^{4}He ratios of 56.0 ± 0.6 Ra and 50.9 ± 1.9 Ra. For these samples, ^{3}He concentration does not correlate with ^{3}He/^{4}He, as might be expected if fluid-inclusion abundances (in olivines with uniform radiogenic ^{4}He) controlled isotopic compositions. Assuming the differences among these three samples reflect magmatic isotopic variability, intraflow ^{3}He/^{4}He variability exceeded 12 Ra.

^{3}He/^{4}He may have decreased over time in Baffin Island magmas. The two samples with the highest He concentrations (PING18-H18 and DURB18-H7) yielded intermediate weighted mean ^{3}He/^{4}He of 43.1 ± 1.0 Ra and 48.3 ± 0.8 Ra. This is consistent with previous studies that recovered the most ^{4}He per gram from Baffin Island olivines with 39–46 Ra (refs. 14,15). Assuming that these intermediate values represent fluid-inclusion-rich olivine rims, magmatic ^{3}He/^{4}He may have decreased from >65 Ra to <50 Ra by the time fluid-inclusion-rich olivine rims grew. This is consistent with the finding that the highest ^{3}He/^{4}He in a given stratigraphic sequence (RB18-H2, PING18-H2 and DURB18-H7) is measured in the oldest lavas[17] and that ^{3}He/^{4}He generally decreases upwards in each section. Isotopic heterogeneity in the plume, assimilation of depleted mantle (about 8 Ra) by the ascending plume, or a flux of externally derived carbon dioxide that delivered non-plume He into the system might explain these observations.

Sr–Nd–Pb isotopes

Whole-rock powders were leached in 6.2 N hydrochloric acid for 1 h at 100 °C and dissolved in 3:1 mixture of concentrated HF:HNO_3, followed by three dry-downs in 6.2 N hydrochloric acid to convert fluorides to chlorides. Separation of Sr and Nd was carried out with Eichrom Sr-Spec and Ln-Spec resin, respectively. Lead was separated following the HBr–HNO_3 procedure of ref. 58 using a single-column pass. Isotopes of Sr, Nd and Pb isotopes were measured on a NEPTUNE multi-collector ICP-MS at WHOI. For Sr and Nd, the internal precision was 10–20 ppm (2σ); external precision, after adjusting to 0.710240 and 0.512104 for the SRM987 Sr and JNdi-1 Nd standards, respectively, was estimated to be 15–25 ppm (2σ). The internal precision for ^{206,207,208}Pb/^{204}Pb ratios was 15–50 ppm; SRM997 Tl was used as an internal standard, and external reproducibility ranges from 17 ppm (2σ) for ^{207}Pb/^{206}Pb, to 120 ppm (2σ) for ^{208}Pb/^{204}Pb. Pb isotope ratios are adjusted to the SRM981 values of ref. 59. The results are reported in Supplementary Table 2.

Radiogenic isotope models

^{87}Sr/^{86}Sr, ^{143}Nd/^{144}Nd and ^{206}Pb/^{204}Pb of Baffin Island lavas at the time of eruption (about 61 million years ago) were estimated as follows:

$$\left[\frac{D}{d}\right]_0 = \left[\frac{D}{d}\right] - \left[\frac{P}{d}\right](e^{\lambda t} - 1)$$

where P is the parent isotope, D is the radiogenic daughter isotope and d is the non-radiogenic isotope of the daughter element. Time (t) is 61 Myr and λ is the decay constant for P (ref. 60). Rb/Sr, Sm/Nd and U/Pb are assumed to be 0.004, 0.347 and 0.072, respectively, based on typical compositions of Baffin Island lavas.

We model binary mixing between DMM endmembers and primordial mantle (PM) with the composition of bulk silicate Earth (Extended Data Fig. 2) as follows:

$$\left[\frac{D}{d}\right]_{mix} = \frac{X_{DMM}[C]_{DMM}\left[\frac{D}{d}\right]_{DMM} + (1 - X_{DMM})[C]_{PM}\left[\frac{D}{d}\right]_{PM}}{X_{DMM}[C]_{DMM} + (1 - X_{DMM})[C]_{PM}}$$

where X_{DMM} is the weight fraction of DMM and [C] is the abundance of the daughter element in each component. We assume that reasonable depleted mid-ocean ridge mantle isotopic and elemental compositions fall within the depleted (D-DMM), average (A-DMM) and enriched (E-DMM) members defined by ref. 25. Primitive mantle ^{87}Sr/^{86}Sr and ^{143}Nd/^{144}Nd[25], as well as ^{206}Pb/^{204}Pb (ref. 61), are considered to be chondritic. ^{87}Sr/^{86}Sr, ^{143}Nd/^{144}Nd and ^{206}Pb/^{204}Pb of DMM and PM were corrected for 61 Myr of ingrowth as described above. We assume that DMM ^{3}He/^{4}He is 8 times the atmospheric ratio (Ra: 1.384×10^{-6}) and that primordial mantle is either 70 Ra or 100 Ra. DMM contains approximately 3×10^{-11} cm^3 ^{3}He STP g^{-1} (ref. 52) and we assume that primordial mantle contains 8×10^{-9} cm^3 ^{3}He STP g^{-1}, the minimum required by the highest ^{3}He/^{4}He in Baffin Island lavas (see main text for details).

^{3}He/^{22}Ne systematics

Solubility and diffusion might influence ^{3}He/^{22}Ne in Baffin Island olivines. Solubility can be ruled out as the primary cause of high and variable time-integrated ^{3}He/^{22}Ne for two reasons. First, inter-element (Ar–Ne–He) isotopic ratios in Baffin Island olivines indicate that gases were trapped in closed-system equilibrium with the magmas[16]. The difference in solubility between He and Ne is at most about two, so closed-system behaviour is not expected to cause extreme elemental fractionation[4]. Second, time-integrated mantle source ^{3}He/^{22}Ne ratios are calculated based on extrapolated ^{21}Ne/^{22}Ne and measured ^{3}He/^{4}He, so they are independent of the measured ^{3}He/^{22}Ne ratios in olivines[4].

Faster He diffusion than Ne diffusion through olivine might influence the measured ^{3}He/^{22}Ne ratios. For example, He may diffuse through olivines under magmatic conditions, causing isotopic equilibration of olivine-hosted fluid inclusions with surrounding magmas or fluids[62]. In contrast, Ne (which diffuses five orders of magnitude slower than He through olivine at upper-mantle conditions[49]) in fluid inclusions probably retains the isotopic composition of the magmatic system when the olivine grew. Increasing ^{3}He/^{22}Ne above that of the mantle source might have occurred in Baffin Island olivines if the magmatic ^{3}He/^{4}He increased after olivines captured fluid and melt inclusions. For instance, flushing of a magma with high-^{3}He/^{4}He carbon-dioxide-rich fluids could increase ^{3}He/^{22}Ne in olivine-hosted fluid inclusions. However, ^{3}He/^{4}He ratios in Iceland plume-derived magmas might be expected to decrease over time due to magma mixing and crustal assimilation[19] because the upper convecting mantle and the crust have much lower ^{3}He/^{4}He than the Iceland plume.

Nucleogenic neon production

Nucleogenic Ne is produced by the capture of α-particles emitted by ^{232}Th, ^{235}U and ^{238}U series isotopes. The reactions that are potentially important in geologic reservoirs include ^{17,18}O(α,n)^{20,21}Ne, ^{19}F(α,n)^{22}Na(β +)^{22}Ne and ^{19}F(α,p)^{22}Ne, as well as ^{24,25}Mg(n,α)^{21,22}Ne and ^{23}Na(n,α)^{20}Ne caused by secondary neutrons[63]. Although the composition of the core remains controversial, it is not expected to contain appreciable fluorine, magnesium or sodium[64], so we only consider the reactions in which oxygen is the target. The Ne production rates per gram of target element in the crust and mantle are nearly equivalent[65]. The stopping power of α-particles is higher in the core than in the mantle and crust due to higher densities, so α-particle energies decrease on shorter length scales. However, higher densities also correspond to more target nuclei near the source, assuming uniform distributions of target elements. Therefore, we assume that the α-particles produced per unit of oxygen in the crust and mantle are reasonable approximations for the core. More recent estimates for nucleogenic

Ne production in silicate minerals[66] are within about 10% of these assumed rates.

The production rate $P(t)$ of a Ne isotope (i) can be expressed as[47]:

$$P(t) = \frac{\mathrm{d}(i)}{\mathrm{d}t} = i_{232}\lambda_{232}[^{232}\mathrm{Th}]e^{\lambda_{232}(T-t)} + i_{235}\lambda_{235}[^{235}\mathrm{U}]e^{\lambda_{235}(T-t)} + i_{238}\lambda_{238}[^{238}\mathrm{U}]e^{\lambda_{238}(T-t)}$$

where i_{232}, i_{235} and i_{238} are the production rates[65] of isotope i per gram of oxygen in the core per decay of ^{232}Th, ^{235}U and ^{238}U, respectively. λ_{232}, λ_{235} and λ_{238} are the decay constants and [^{232}Th], [^{235}U] and [^{238}U] are the present-day concentrations of ^{232}Th, ^{235}U and ^{238}U. T is the age when the system began (assumed to be 4.55 billion years ago) and t is the elapsed time after time T.

To estimate the maximum nucleogenic Ne production, we assume the highest oxygen contents (4 wt%) estimated for the core[41] and initial Th and U of 1.2×10^{-8} mol kg^{-1} and 9.1×10^{-10} mol kg^{-1} (ref. 37), respectively. We further assume initial solar ^{20}Ne/^{22}Ne, ^{21}Ne/^{22}Ne and ^{3}He/^{20}Ne of 13.26, 0.0329 and 0.3 (ref. 40). In a core with ^{3}He abundances high enough to preserve the highest ^{3}He/^{4}He observed in Baffin Island lavas (>65 Ra), the nucleogenic Ne accumulation would not detectably change the ^{20}Ne/^{22}Ne or ^{21}Ne/^{22}Ne. For example, if there is 8×10^{-11} cm^3 ^{3}He STP g^{-1} (corresponding to 3×10^{-10} cm^3 STP g^{-1} of Ne), less than three parts per thousand of ^{21}Ne in the core (and much less ^{20}Ne and ^{22}Ne) would be nucleogenic. The production ratio of ^{21}Ne/^{4}He is about 4×10^{-9}, or roughly one order of magnitude less than in silicate minerals[66], owing to the much lower oxygen abundance in the core.

Data availability

All data are available in the paper, the supplementary materials and on EarthChem (https://doi.org/10.26022/IEDA/112776).

54. Kurz, M. D. et al. Correlated helium, neon, and melt production on the super-fast spreading East Pacific Rise near 17°S. *Earth Planet. Sci. Lett.* **232**, 125–142 (2005).
55. Kurz, M. D., Curtice, J., Fornari, D., Geist, D. & Moreira, M. Primitive neon from the center of the Galápagos hotspot. *Earth Planet. Sci. Lett.* **286**, 23–34 (2009).
56. Patterson, D. B., Farley, K. A. & McInnes, B. I. A. Helium isotopic composition of the Tabar–Lihir–Tanga–Feni island arc, Papua New Guinea. *Geochim. Cosmochim. Acta* **61**, 2485–2496 (1997).
57. Scarsi, P. Fractional extraction of helium by crushing of olivine and clinopyroxene phenocrysts: effects on the ^{3}He/^{4}He measured ratio. *Geochim. Cosmochim. Acta* **64**, 3751–3762 (2000).
58. Abouchami, W., Galer, S. J. G. & Koschinsky, A. Pb and Nd isotopes in NE Atlantic Fe–Mn crusts: proxies for trace metal paleosources and paleocean circulation. *Geochim. Cosmochim. Acta* **63**, 1489–1505 (1999).
59. Todt, W., Cliff, R. A., Hanser, A. & Hofmann, A. W. In *Earth Processes: Reading the Isotopic Code* (eds. Basu, A. & Hart, S.) 429-437 (American Geophysical Union, 1996).
60. Dickin, A. P. *Radiogenic Isotope Geology* (Cambridge Univ. Press, 2018).
61. Maltese, A. & Mezger, K. The Pb isotope evolution of bulk silicate Earth: constraints from its accretion and early differentiation history. *Geochim. Cosmochim. Acta* **271**, 179–193 (2020).
62. Horton, F., Farley, K. & Jackson, M. Helium distributions in ocean island basalt olivines revealed by X-ray computed tomography and single-grain crushing experiments. *Geochim. Cosmochim. Acta* **244**, 467–477 (2019).
63. Yatsevich, I. & Honda, M. Production of nucleogenic neon in the Earth from natural radioactive decay. *J. Geophys. Res. Solid Earth* **102**, 10291–10298 (1997).
64. McDonough, W. F. Compositional model for the Earth's core. *Treatise Geochem.* **2**, 547–568 (2003).
65. Leya, I. & Wieler, R. Nucleogenic production of Ne isotopes in Earth's crust and upper mantle induced by alpha particles from the decay of U and Th. *J. Geophys. Res. Solid Earth* **104**, 15439–15450 (1999).
66. Cox, S. E., Farley, K. A. & Cherniak, D. J. Direct measurement of neon production rates by (α, n) reactions in minerals. *Geochim. Cosmochim. Acta* **148**, 130–144 (2015).

Acknowledgements M. Mahy of Parks Canada Nunavut Field Unit assisted with fieldwork planning. V. Hooten performed mineral separation. N. Chatterjee carried out electron microprobe analyses. This research was funded by the National Science Foundation (award number 1911699). The Woods Hole Oceanographic Institution Andrew W. Mellon Foundation Endowed Fund for Innovative Research and a National Geographic Society grant (CP4-144R-18) supported fieldwork activities.

Author contributions F.H.: conceptualization, methodology, investigation, writing—original draft, visualization, supervision, and funding acquisition. P.D.A.: conceptualization, investigation, resources, writing—review and editing, supervision, and funding acquisition. K.A.F.: conceptualization, methodology, investigation, resources, writing—review and editing, supervision, and funding acquisition. J.C.: methodology and investigation. M.D.K.: resources, methodology, writing—review and editing, and supervision. J.B.: methodology, investigation, resources, writing—review and editing. J.A.B.: investigation. X.M.B.: formal analysis and investigation.

Competing interests The authors declare no competing interests.

Additional information

Supplementary information The online version contains supplementary material available at https://doi.org/10.1038/s41586-023-06590-8.

Correspondence and requests for materials should be addressed to F. Horton.

Peer review information *Nature* thanks David Graham and the other, anonymous, reviewer(s) for their contribution to the peer review of this work.

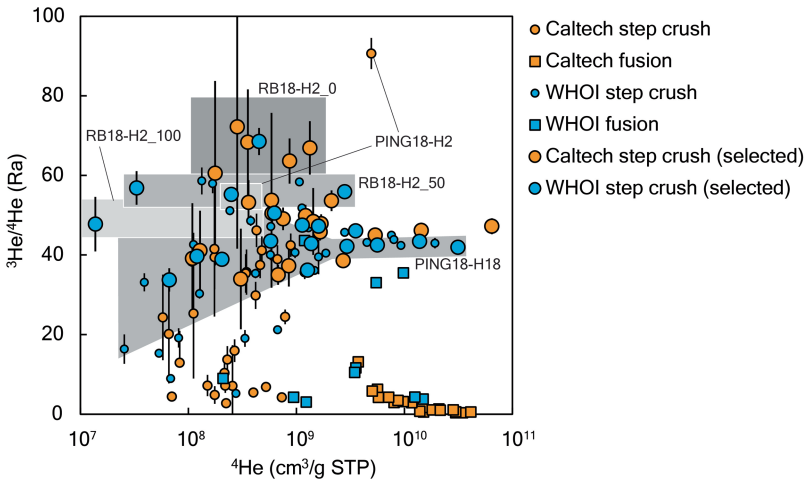

Extended Data Fig. 1 | ^{3}He/^{4}He as a function of ^{4}He/g. Most fusion analyses yielded low ^{3}He/^{4}He ratios and high He abundances, which is consistent with the presence of radiogenic ^{4}He in the matrix of the olivines. The highest gas yields during crushing were for samples with abundant olivine-hosted fluid inclusions and have ^{3}He/^{4}He of 40–50 Ra. Error bars (1 s.d.) are shown where uncertainty is larger than the symbols.

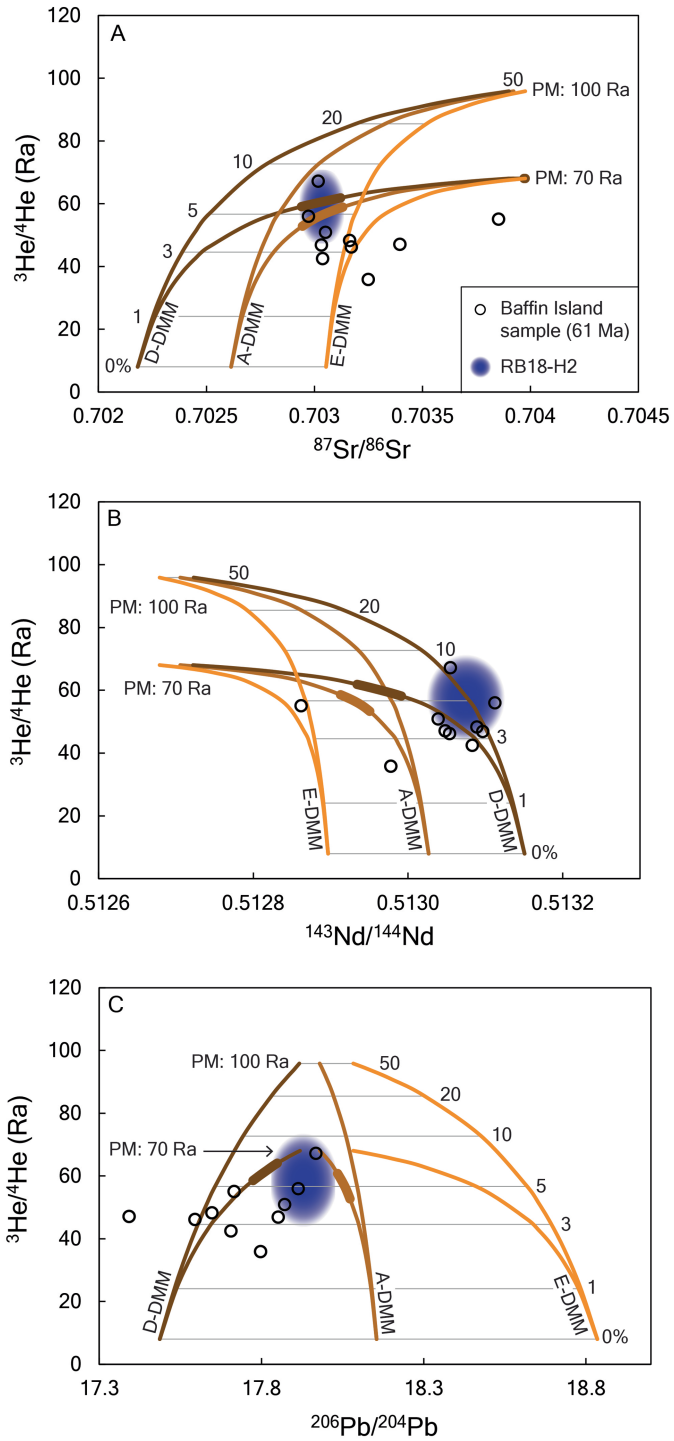

Extended Data Fig. 2 | Primordial and depleted mantle mixing models. Binary mixtures of depleted mid-ocean ridge basalt mantle (DMM) and primitive mantle (PM) of bulk silicate Earth composition cannot explain the isotopic compositions of the lava flow with the highest reproducible ^{3}He/^{4}He (RB18-H2), which we assume represents the highest ^{3}He/^{4}He mantle component in Baffin Island lavas. Plausible compositions are bracketed by depleted (D-DMM), average (A-DMM), and enriched (DMM) endmembers. Corresponding segments of two mixing lines are thickened to highlight this discrepancy. Each endmember and the Baffin Island data are corrected for radiogenic ingrowth of Sr, Nd, and Pb since 61 Ma. See Methods for details.

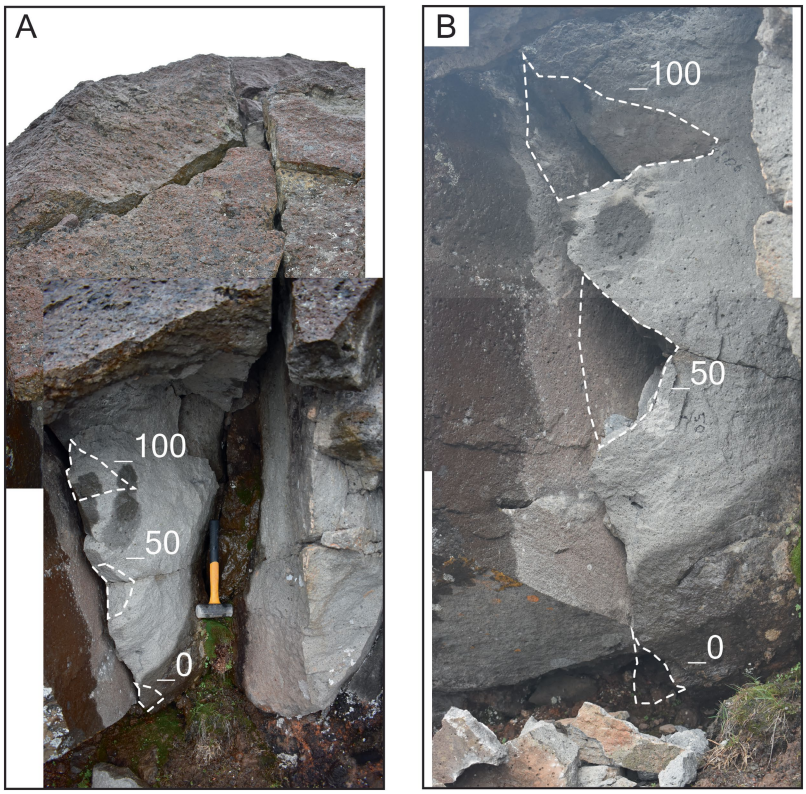

Extended Data Fig. 3 | RB18-H2 sampling site. Before (A) and after (B) photograph montages of the sampling site for samples RB18-H2_0, RB18-H2_50, and RB18-H2_100. All three samples are from the base of the flow, which is greater than 4 m thick. RB18-H2_50 and RB18-H2_100 were sampled 50 cm and 100 cm above the base of the flow, respectively. All three samples are from minimally weathered surfaces beneath an overhang, where they were shielded from cosmic rays. In these images, the lighter portion of the outcrop is dry because it is beneath the overhang and therefore less exposed to rainwater. Dashed white lines indicate the approximate location of each sample. See the 6 lb. hammer for scale.

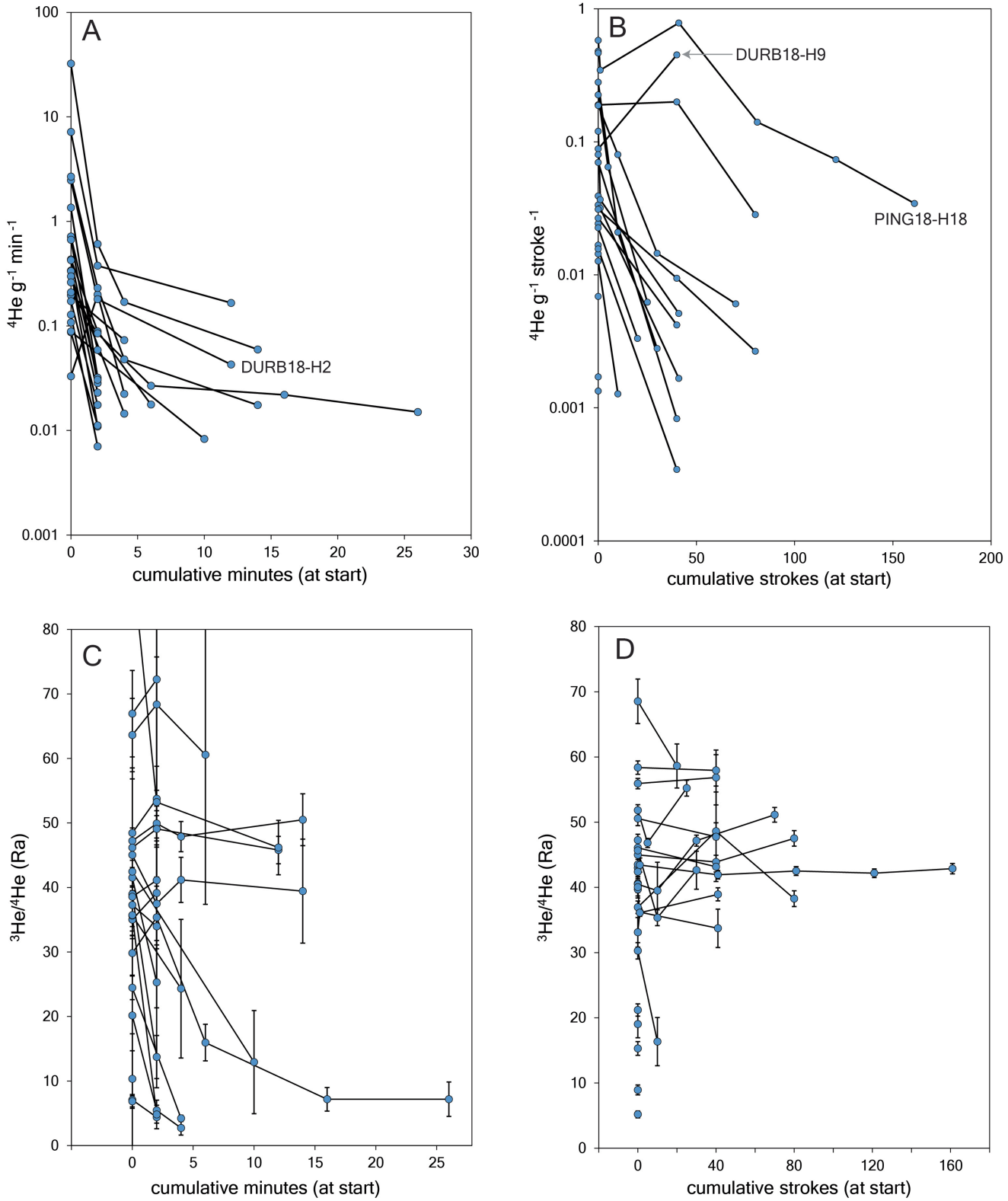

Extended Data Fig. 4 | Helium yields from crushing experiments. In most cases, He yields decreased over time during Caltech (A) and WHOI (B) step crushing experiments. Because the automated crushing intervals and numbers of strokes per extraction varied among experiments, the He yields are normalized to mass and minutes of crushing in panel (A) and to mass and crushing strokes in panel (B). Tie lines connect individual measurements for single mineral separates. Anomalous experiments for which ^{4}He increased over time are labeled. ^{3}He/^{4}He changes across crushing steps were less systematic, but mostly stayed relatively constant or decreased over time at Caltech (C) and WHOI (B). The ^{3}He/^{4}He decreases were most pronounced at Caltech.

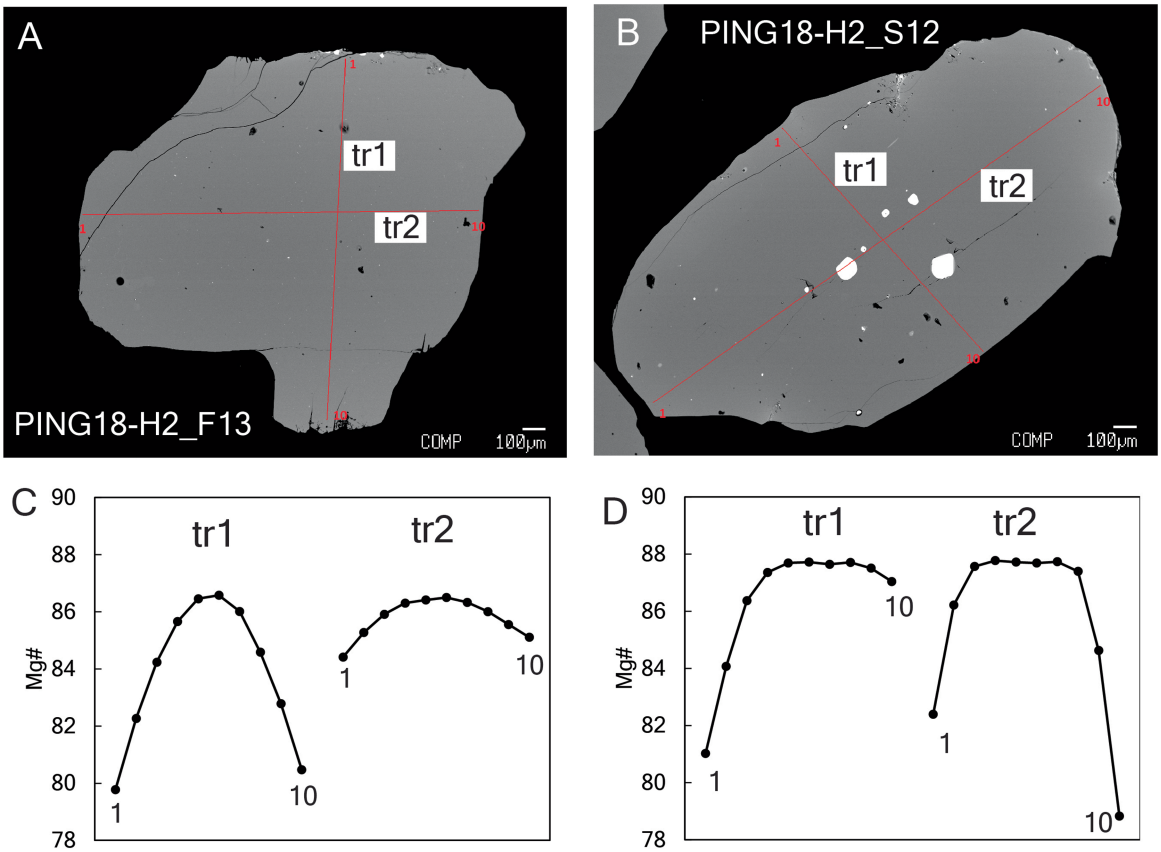

Extended Data Fig. 5 | Olivine zoning. Mg#, Ni, and Cr increase from rim to core in Baffin Island olivines. In spinel-rich olivine cores, the abundance of these elements extends to higher levels (Mg# > 87.5, Ni > 4.5 wt%, and Cr > 0.14 wt% in most grains) than in fluid inclusion-rich olivine rims. Mn profiles exhibit the opposite trend and zoning is less systematic with respect to Al and Ca. The two olivine populations—spinel-rich and fluid inclusion-rich—have overlapping Mg#, Ni, and Cr that are offset to lower values for fluid inclusion-rich grains by ~1, 0.5 wt%, and 0.2 wt%, respectively. Shown here are representative electron probe micro analyzer (EPMA) transects across a fluid inclusion-rich olivine (A and C) and a spinel-rich olivine (B and D). Both olivines are from sample PING18-H2. In A and B, backscatter electron images show the location of EPMA transects and the distribution of inclusions on the polished surface of the grain. In A, most inclusions are fluid inclusions (black). In B, the olivine has large spinel inclusions in its core (white) and some fluid inclusions (black). In both grains, the Mg# (100 × MgO / [MgO + FeO]) is greatest in the core and decreases towards the rim. Spinel-bearing olivines have higher Mg# in their cores than fluid inclusion-rich olivines without spinel. Some grains have spinel cores overgrown by lower Mg# rims that contain fluid inclusions. Complete EPMA data are available in SI Table 3.

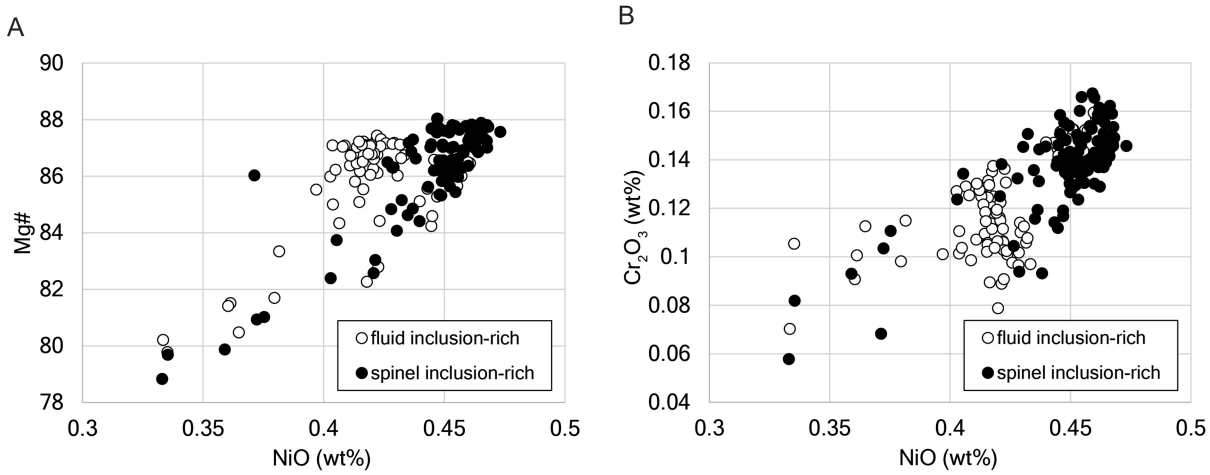

Extended Data Fig. 6 | Olivine compositions. Fluid inclusion-rich and spinel-rich olivine grains have overlapping compositions. In general, Mg#, NiO, and CrO are higher for spinel-rich olivines domains.

Extended Data Table 1 | Reproducible $^{3}He/^{4}He$ crushing results

Sample	$^{4}He/g$ (10^{-9} cm^{3}/g STP)	$^{3}He/^{4}He$ (Ra)	SE	n
DURB18-H7	17.0	48.3	0.8	4
DURB18-H8	4.5	47.1	0.7	4
DURB18-H9	1.9	46.2	2.4	3
DURB18-H10	0.5	35.9	1.5	4
PING18-H2	0.3	55.1	1.3	2
PING18-H3	3.5	46.9	1.3	2
PING18-H18	9.3	42.5	0.3	6
RB18-H1	0.8	39.1	0.3	4
RB18-H2_0	0.6	67.2	1.8	6
RB18-H2_50	1.4	56.0	0.6	2
RB18-H2_100	0.9	50.9	1.9	3
RB18-H3	0.6	36.8	2.0	2

Twelve samples have $^{3}He/^{4}He$ values that overlap within 1SD analytical uncertainty. The reported means for these samples are inverse-variance weighted and assigned weighted standard errors. Due to possible radiogenic ^{4}He contributions, these results should be viewed as minimum magmatic ratios. See Supplementary Table 1 for complete He results.